Available online at www.sciencedirect.com
SCIENCE DIRECT®

Catalysis Today 116 (2006) 324–333

CATALYSIS TODAY

www.elsevier.com/locate/cattod

Design of a diesel reformer coupled to a PEMFC

F. Rosa [a,*], E. López [a], Y. Briceño [b], D. Sopeña [b], R.M. Navarro [c], M.C. Alvarez-Galván [c], J.L.G. Fierro [c], C. Bordons [d]

[a] *Instituto Nacional de Técnica Aeroespacial, Centro de Experimentación de Arenosillo, Ctra San Juan Matalascañas, Km. 33, 21130 Mazagón, Huelva, Spain*
[b] *CIDAUT, Parque Tecnológico Boecillo, Valladolid, Spain*
[c] *Instituto de Catálisis y Petroleoquímica (CSIC), Cantoblanco, Madrid, Spain*
[d] *Escuela Superior de Ingenieros, Sevilla, Spain*

Abstract

A strategic alliance has been established between Spanish partners to develop a 5 kW diesel fuel processor for an integrated operation with a PEMFC. Oxidative Steam Reforming followed by a novel WGS reactor in one step and a PROX delivers a stream with a maximum CO of 20 ppm, able to feed PEM without poisoning the anodes. Paper presents a detailed description of the work carried out to obtain novel catalyst (main section of this paper), design of the reformer and preliminary operational results. Data concerning how catalysts were prepared and catalytic activity measurements for OSR, WGS and PROX is presented as well design of test bench and control. From an experimental point of view some results, at laboratory scale, are presented concerning OSR, WGS and PROX and as well preliminary results concerning global operation of the prototype.

Keywords: Diesel; Reformer; PEMFC

1. Introduction

Several studies have shown that fuel cells can contribute to solve global warming issues of the planet, using in a rational ways fossil fuels and, additionally, will improve energy efficiency of power cycles. However at present, hydrogen storage technologies are not enough mature to store acceptable energy densities; so that, liquids fuels will have to be the energy carriers in many applications at short term. The fuel processor represents therefore the link between the fuel supply and the fuel cells and its characteristics are defined not only by fuel properties but also by the requirements of the fuel cell stack. Between fuels examined as feedstocks for fuel processor, diesel fuel has been considered as results of its high gravimetric and volumetric hydrogen density and a well-established delivery infrastructure. In an initial step, we have carried out the design and construction of a diesel reformer prototype capable to fulfil hydrogen need of a PEMFC of 5 kW. On this prototype we plan to acquire the experience to proceed in a future scale up to 20 kW power system. To carry out involved tasks, INTA has established strategic alliances with well-recognised Spanish partners with experience in selected knowledge areas: catalyst (Institute of Catalysis and Petroleochemistry of CSIC), control (AICIA) and chemical reactor design (CIDAUT). In an initial step, system has been designed to fulfil hydrogen need of a PEMFC of 5 kW.

The technology to generate hydrogen from diesel includes three basic processes: steam reforming (SR), partial oxidation (PO) and oxidative steam reforming (OSR). Among the aforementioned processes, the oxidative steam reforming is the basic conversion system selected to use in our reformer since it offers a simpler design, a lower temperature of operation and a more dynamic response to work under varying loads. The reforming of diesel fuel for the production of hydrogen is difficult because of the refractory nature of the compounds present in diesel fractions [1]. The catalysts for diesel reforming must be carefully formulated to achieve resistance to high temperatures, sulphur poisoning and coke deposition. Catalyst formulations typically comprise [2,3] noble (Pt, Rh and Ru) or

---

[*] Corresponding author.
E-mail address: rosaif@inta.es (F. Rosa).

0920-5861/$ – see front matter © 2006 Elsevier B.V. All rights reserved.
doi:10.1016/j.cattod.2006.05.061

non-noble metals (Ni and Co) deposited or incorporated into carefully engineered supports (thermal stabilized alumina, doped alumina with promoters to accelerate coke gasification, mixed metal oxides, oxide-ion conducting substrates, . . .). Perovskite type catalysts (lanthanum cromites and alumites) have been also explored with success as alternative formulation for the catalytic oxidative reforming of diesel fuel [4]. For this work, we are developing diesel reforming catalysts based on: (i) transition metals (Pt, Ru, Co and Ni) supported of Al_2O_3 substrates promoted with different elements (Mg and lanthanides) to improve both thermal robustness and sulphur and coke tolerance, (ii) transition metal (Co) based perovskite compounds (with La) and (iii) transition metals (Ru, Pt) supported on mixed oxides with perovskite structure (La–Co perovskite).

Depending on the design and operating conditions of the reformer, the H_2-rich effluent gas contains 5–10 vol.% of carbon monoxide. This carbon monoxide must be converted in additional hydrogen in order to increase the efficiency of the reforming process and to avoid the rapid deactivation of electro-catalysts in the fuel cell. For this purpose, a water gas shift and subsequent CO preferential oxidation reactors were integrated after the primary reformer unit. Taking into account that WGS in the reformer will suffer many start-up/shutdown cycles, it was objective of the project to develop alternative WGS catalysts with similar activity for CO conversion than that obtained with commercial WGS systems but overcoming: (i) the necessity of two stages for CO conversion, (ii) the careful activation step and, (iii) the deactivation against air and water condensation. Among the various metal–support combinations examined in the literature [5–7], platinum and gold particles supported on reducible oxides are particularly active for the WGS reaction. However, the stability under reaction conditions is the main drawback with using the above catalytic systems in WGS applications. For the design of active WGS catalysts to be used in the reformer, we have combined several factors: nature of active phase (Pt and Au), metal loading, type of support (CeO_2, TiO_2, Al_2O_3 and their mixtures) and preparation methods (impregnation, deposition–precipitation and coprecipitation).

Respect to catalyst formulations active in the CO preferential oxidation (PROX), the literature cites several oxidation catalysts that show selectivity in the presence of hydrogen. These systems include platinum, copper, ruthenium and gold [8–10] deposited on various oxide supports. Except for the industrial application of Pt–Fe supported catalysts developed by Engelhart, there is not a catalyst formulation that showed a clear advantage over the rest of published formulations. For this reason, and in the same way to the screening previously described for WGS catalysts, several metal/support formulations were investigated in order to identify the functionalities, metal and support, that enhances PROX activities in order to be able to optimize a catalytic formulation to be load in the reformer. In the present project we have explored the catalyst performances of Au and Pt based supported catalysts on several oxides substrates (Al_2O_3, TiO_2, zeolites, CeO_2 and their mixtures) using different methodologies of preparation.

A model to obtain the necessary information in the design phase of different components in reforming installations has been developed. The Lagrangian approach, in which this model is based, allows to obtain a one-dimensional resolution on steady state conditions, being easily applicable to other kind of reformer technologies to generate hydrogen [11–14]. In the developed code implemented in the model, expressions that govern the miscellaneous equipment behaviour are included, as well as the chemical kinetic equations and mass and energy balances. Fig. 1 shows some simulation results of the different reactors used in the system design. Gas composition and temperatures along each reactor can be observed. Must be stated that these results does not

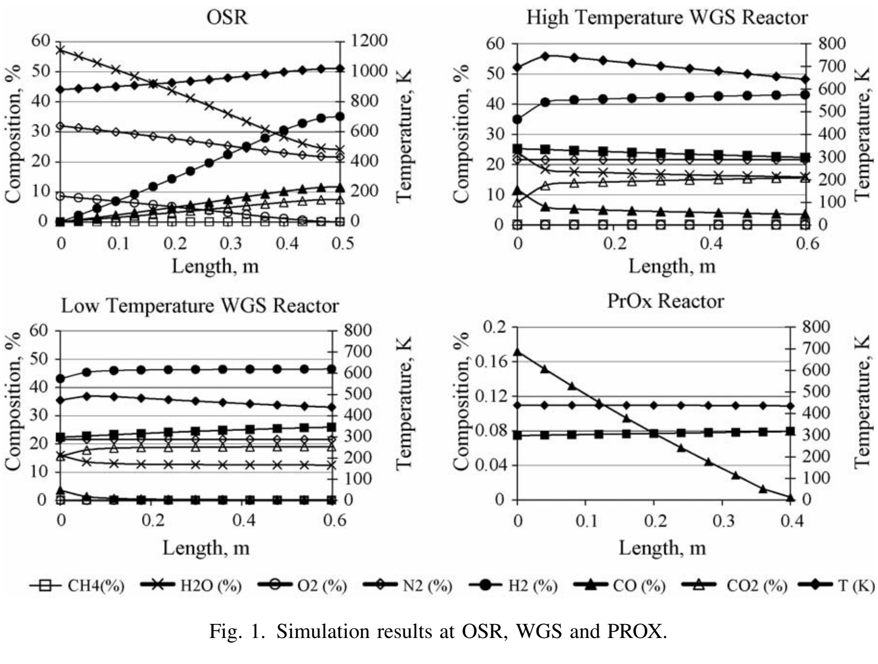

Fig. 1. Simulation results at OSR, WGS and PROX.

take into account the final reactor design (one WGS step instead of the classical two steps).

Control features, operation procedure and fuel processor P&I of the reformer have been previously published [15].

2. Experimental

2.1. Catalysts preparation

2.1.1. Diesel reforming catalysts

The Al_2O_3 support (γ, bimodal, Johnson Matthey) was crushed and sieved to a particle size between 0.20 and 0.42 mm and stabilized by calcination at 1273 K for 8 h. The lanthanide structural promoters (L1) were introduced into non-stabilized alumina by incipient wetness pore volume impregnation with aqueous solutions of promoter nitrates. After impregnation, the doped alumina was dried at 383 K and subsequently calcined at 1273 K over 8 h. Activity promoters (alkaline and lanthanides) were deposited by impregnation of bare alumina (calcined at 1273 K for 8 h) or doped alumina with the appropriate amount of an aqueous solution of metal nitrates in a rotary evaporator at 353 K for 2 h. After impregnation, the supports were dried at 383 K for 8 h and calcined at 773 K for 4 h. Table 1 shows the nominal chemical composition and surface areas of the different supports prepared. Specification of the nature of the lanthanide and alkaline elements was not possible because of patent application. Supported nickel (4–10 wt.% NiO, nominal), platinum (1–6 wt.% Pt, nominal) and ruthenium (1–10% Ru, nominal) catalysts were prepared by impregnation of the modified alumina previously described. For this purpose, appropriate amounts of $Ni(NO_3)_2{\cdot}6H_2O$ (crystal, Aldrich), H_2PtCl_6 (Johnson Matthey) and $RuCl_3$ (Johnson Matthey) were used to obtain the supported catalysts by wet impregnation. All samples were dried at 383 K for 4 h and calcined at 773 K for 3 h.

Perovskite oxides (ABO_3) precursors (A = Co, B = lanthanide) were prepared by citrate method using equimolar A and B nitrates mixtures. After precipitation, the solid was dried at 393 K and then calcined at 1073 K for 4 h. Noble metals (Ru, Pt) were added (0.2 mol%, nominal) to ABO_3 perovskite by means of aqueous impregnation. After noble metal loading, the samples were dried at 393 K and subsequently calcined at 773 K.

2.1.2. Water gas shift catalysts

The titania support (catalyst support Alfa Aesar 150 m^2/g BET area) was stabilized by thermal treatment at 773 K for 4 h. High surface area ceria support was prepared by the urea coprecipitation–gelation method. Following the precipitation, ceria was dried at 383 K for 4 h and, finally calcined in air at 923 K for 8 h. Mixed ceria–titania supports (CeO_2: 3–15 wt.%) were prepared by impregnation of the calcined. Table 1 collects nominal chemical composition and surface areas of the different prepared supports. Supported Pt and Au catalysts were prepared by impregnation of each of the above supports, under stirring at 343 K for 2 h using aqueous solutions of H_2PtCl_6 and $HAuCl_4$ metal precursors. After metal loading (0.25–1 wt.% Pt and 0.5–1 wt.% Au), the samples were dried in air at 383 K, followed by calcination in air at 773 K for 3 h.

2.1.3. Preferential oxidation catalysts

Commercial TiO_2 (Alfa Aesar), Al_2O_3 (Johnson Matthey), and ZSM-5 were used as catalysts supports without any pre-treatment before impregnation. Mixed CeO_2–Al_2O_3 (CeO_2: 5–20 wt.%, nominal) supports were prepared by impregnation of alumina with the appropriate amount of an aqueous solution of cerium nitrate ($Ce(NO_3)3{\cdot}6H_2O$, 99.9%, Johnson Matthey) in a rotary evaporator at 353 K for 2 h. Table 1 collects nominal compositions and surfaces areas of the different supports studied.

Supported Pt (0.5–5 wt.%) and Au (0.5–5 wt.%) catalysts were prepared by impregnation of each of the above supports, under stirring at 343 K for 2 h using aqueous solutions of H_2PtCl_6 and $HAuCl_4$ metal precursors. After metal loading, the samples were dried in air at 383 K, followed by calcination in air at 773 K for 3 h.

2.2. Catalytic activity measurements

The individual behaviour of catalysts developed for each unit was studied using reactors at laboratory scale. These

Table 1
Chemical composition (wt.%) and BET surface areas of supports used in the oxidative reforming, water gas shift and preferential oxidation catalysts

	% Alkaline oxide	% Lanthanide oxide 1	% Lanthanide oxide 2	% CeO_2	% BET (m^2/g)
A[a]					83
A–L1[a]		3–20			104–68
A–L2[a]			5–20		80–40
A–L1–A1[a]	9	3–20			90–60
A–L1–L2[a]		3–20	5–20		70–40
TiO_2[b]					65
CeO_2[b,c]					62
CeO_2–TiO_2[b]				3–15	63–50
Al_2O_3[c]					165
TiO_2[c]					150
Al_2O_3–CeO_2[c]				3–20	161–110

[a] Used in preferential oxidation catalysts.

[b] Used in WGS catalysts.

[c] Used in PROX catalysts.

studies allowed the fast screening of catalysts activities and the determination of both optimal operating conditions and stability of catalysts under working conditions.

2.2.1. Oxidative reforming tests

Oxidative reforming tests were carried out in a fixed-bed continuous-flow stainless steel reactor. Oxidative reforming was studied over both a hydrocarbon mixture that surrogates diesel composition (hexadecane, decaline, tetraline and diesel, 50 ppm S) and commercial low sulphur diesel fuel (15 ppm). Before the reaction, the catalysts were first reduced by H_2/N_2 (1:10, molar ratio) at 623 and 873 K for the platinum-, ruthenium- and nickel-supported catalysts, respectively, over 2 h. For perovskite samples the pre-treatment before catalytic test consisted in a heating to reaction temperature in He flow (50 mL/min). Reforming tests were performed in the temperature range of 923–1173 K, under gas hourly space velocities (GHSVs) ranging between 20,000 and 80,000 h^{-1}, with an $O_2/C/H_2O$ molar feed ratios between 0.2–0.7/1/3–5.

2.2.2. Water gas shift tests (WGS)

Water gas shift tests were carried out in a fixed-bed continuous-flow quartz reactor. Prior to reaction, the catalysts were flushed in nitrogen at 473 K, followed by reduction *in situ* at 548 K for 2 h (heating rate 5 K/min) with 50 mL(STP)/min of a 10 vol.% H_2/N_2 mixture. The catalysts were tested for the water gas shift reaction of gas mixtures simulating typical compositions of reformatted streams (H_2 28%, CH_4 0.1%, CO 4.4%, N_2 29.2%, CO_2 8.7%, H_2O 29.6%). Activity was measured at atmospheric pressure, under a gas hourly space velocity between 12,000 and 48,000 h^{-1} and temperatures between 498 and 573 K, running from the lowest to the highest temperature.

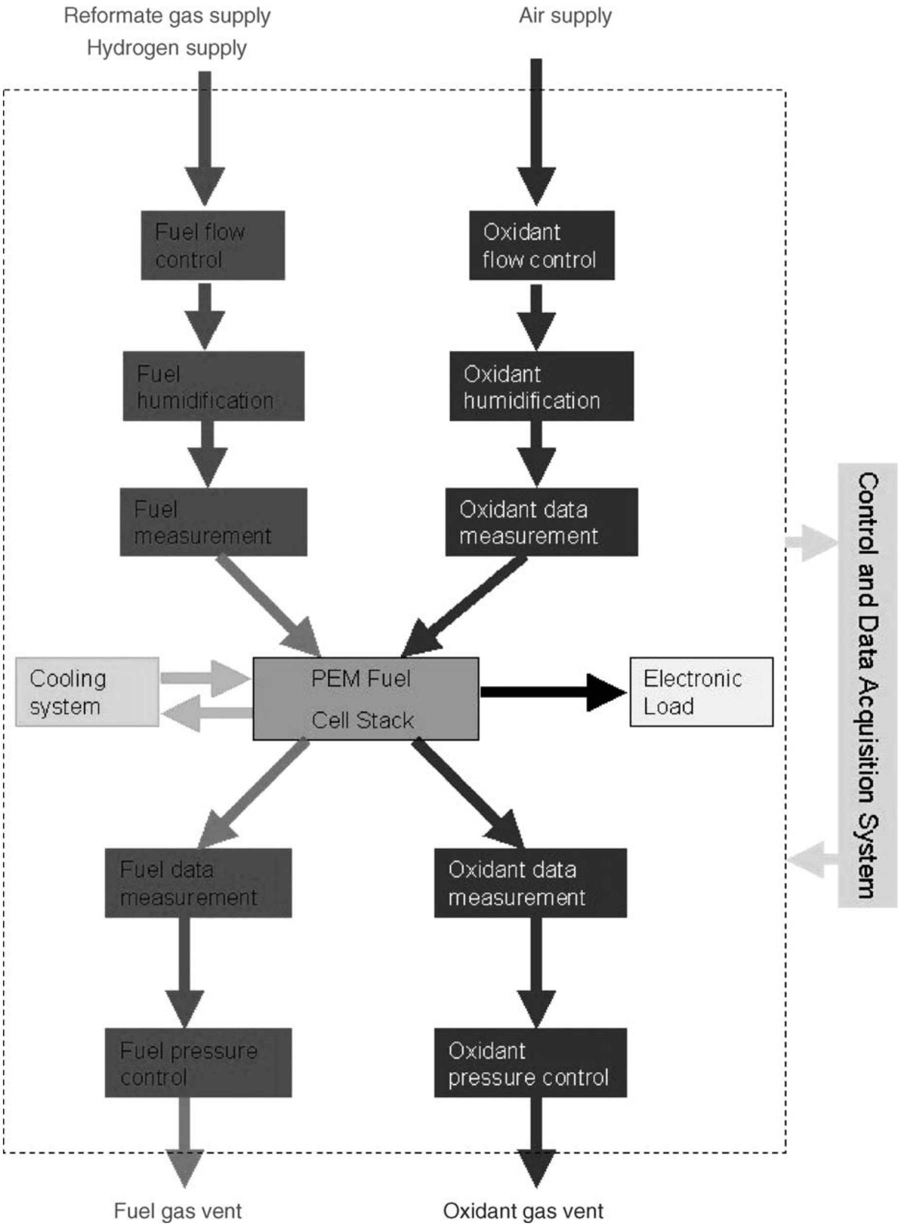

Fig. 2. Fuel cell system boundaries.

2.2.3. Preferential oxidation tests (PROX)

The activity of preferential oxidation catalysts was measured in an atmospheric continuous flow reactor (i.d. 9 mm and 9 cm long) over gas mixtures that simulate the typical stream composition after WGS unit (H_2 33.4 vol.%, CO_2 12.9 vol.%, CO 0.4 vol.%, H_2O 21.7 vol.% and N_2 31.6 vol.%). Catalytic PROX laboratory studies were performed in the temperature range of 323–443 K, space velocity of 3000–13,000 h^{-1} and feed molar ratios of O_2/CO = 0.5–1.0.

2.3. Test bench and control

PEMFC test bench is placed in a building destined to hydrogen technologies and fuel cells and next to diesel reformer. This building comprises three separated rooms: a control room, auxiliary systems room and the laboratory with test bench. PEMFC stack used to be operated with the diesel reformer is a 5 kW nominal power Teledyne Perry 72-cell, supplied by Teledyne Energy Systems and able to operate with 38% of hydrogen content in the reformated gas. Fuel cell system boundaries have been set up according to Fig. 2. Fig. 3 shows main components of diesel reformer prototype: OSR, WGS reactor and PROX. Usually the working pressure is ower than 3 bar, but test bench has been designed to operate at higher pressures (up to 10 bar). The oxidant gas used during normal tests is air, but oxygen supply is also available. Fuel cell stacks are sensitive to contaminants in the form of ions, specifically metal cations, so it is imperative that materials in contact with reactant gases be, in order or precedence: titanium, Teflon, good quality silicon, 316 of better stainless steel, glass, etc. (Fig. 3).

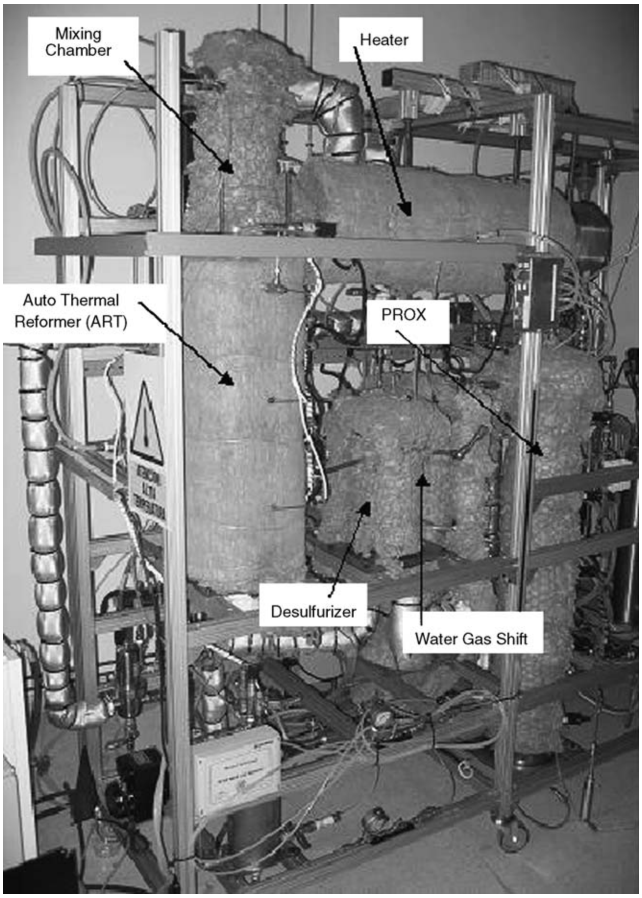

Fig. 3. View of main components of diesel reformer prototype.

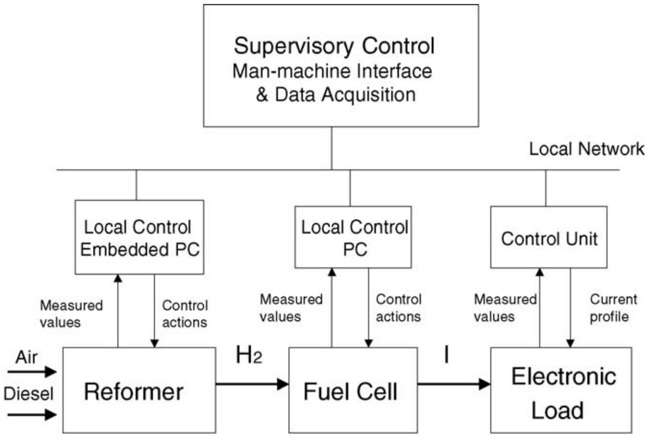

Fig. 4. Schematic layout of the control system.

Electric load is a water-cooled 12,000 W electronic load from TDI, to be used in the range 0–100 V, 0–1000 A. Data acquisition system configuration is based on an external bus connecting a number of distributed data-taker cards with the host computer. Labview based software has been developed for evaluation and surveillance. Abnormal events that should produce any kind of alarm will be also recorded. The coupling between the reformer and the fuel cell has to be carefully designed in order to obtain good performance of the whole system. A two-level control strategy has been devised that allows an integrated control of both parts. The objective of this strategy is to make the system work in the optimum operating point at each instant. The high level (supervisory) control computes the optimal set-points that are sent to the reformer and fuel cell local controllers (low level). This is depicted in Fig. 4. The supervisory control receives information of states of reformer and fuel cell, that it is used with the load demanded at each sampling time, to compute the best operating values for both equipments. Load demand can be detected measuring the electrical current at the fuel cell output or the pressure of the hydrogen supply to the cell. The local controllers of the reformer are PID regulators embedded into a microprocessor board. The optimal control is based on Model Predictive Control (MPC), which solves the optimisation problem on-line. This high level control is also responsible for fault detection and diagnosis.

3. Results

3.1. Laboratory scale testing

3.1.1. Oxidative reforming tests

Preliminary oxidative reforming of hexadecane was performed as screening tests to select both the type and concentration of elements to add to alumina in order to improve its thermal and coke resistance as support of transition metals.

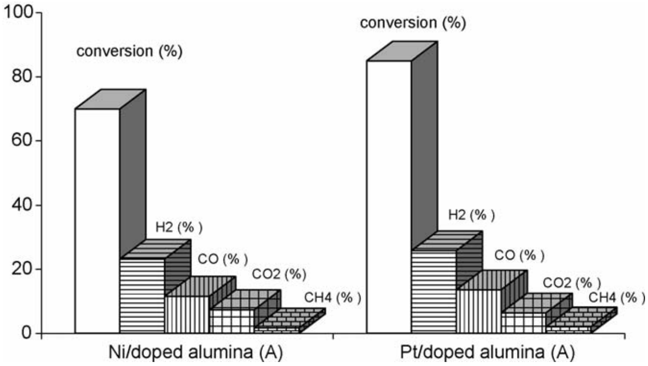

Fig. 5. Conversion and product distribution (mol%, dry) in the oxidative reforming of diesel surrogate (50 ppm S) on Ni and Pt supported on doped alumina. Reaction conditions: $T = 1123$ K, $P = 0.1$ MPa, $O_2/C = 0.5$, $H_2O/C = 3$, GHSV = 20,000 h^{-1}.

First experiments were conducted over Ni (10 wt.% NiO), Ru (1 wt.% Ru) and Pt (1 wt.% Pt) catalysts supported on the different modified alumina (A, A–L1, A–L2, A–L1–A1, A–L1–L2) in order to know the effect of the nature of the support in the catalytic activity. From these experiments it was selected the A–L1–L2 as support of active metal phases taking into account the better results in terms of thermal and coke resistance presented by this support formulation over all active phases tested in the reforming of hexadecane. Fig. 5 shows the conversion and product composition for the oxidative reforming of synthetic mixtures surrogating diesel on catalysts based on different transition metals supported on the A–L1–L2 support. The comparison of hydrogen yields derived from the figure indicated the better performance of Pt based catalyst respect to those obtained on catalysts based on Ni or Ru (not represented in Fig. 5 but showing an extremely low value of conversion). Additionally, the higher CO production on Pt catalyst will imply a higher hydrogen production by the subsequent CO transformation in the water gas shift process.

In a second stage, operation variables were optimized for hydrogen production. The effect of temperature, gas hourly space velocity, oxygen:fuel ratio and water:fuel ratio on hydrogen production was studied. From this study, summarized in Table 2, oxidative reforming over Pt catalysts at 1023 K, under a gas hourly space velocity of 20,000 h^{-1} and feed ratios of $H_2O/C/O_2 = 3/1/0.5$ lead to improved hydrogen productions. Long-term stability of Pt/A–L1–L2 catalyst was determined during 80 h of oxidative reforming of a commercial diesel (15 ppm S) under the above operation conditions. Fig. 6 shows the variations in the conversion and CO and H_2 selectivity as function of time-on-stream. From Fig. 6, it is observed a stable hydrocarbon conversion during this long-time test. Nevertheless, it is observed changes in the concentrations of H_2 and CO in the reformatted gas with the reaction time. The changes are especially significant in the first 20 h of reaction. In this period the hydrogen concentration dropping from 39% to 30% while CO simultaneously increasing from 6% to 10%. After the first 20 h of reaction, the changes in hydrogen and CO concentrations decreased slightly with reaction time. This catalyst deactivation behaviour will imply an over design factor

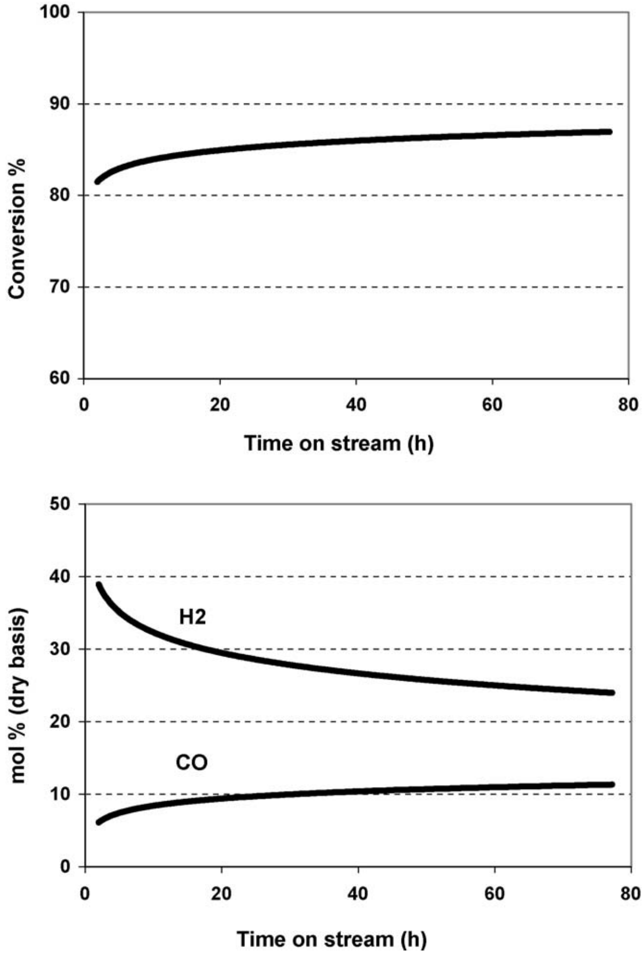

Fig. 6. Stability in the oxidative reforming of commercial diesel (15 S ppm) over Pt supported on doped alumina. Reaction conditions: $T = 1123$ K, $P = 0.1$ MPa, $O_2/C = 0.5$, $H_2O/C = 3$, GHSV = 20,000 h^{-1}.

Table 2
Influence of operation variables on the % of theoretical hydrogen (including WGS of CO coproduced) produced by oxidative reforming of surrogated diesel (50 S ppm) over platinum/doped alumina catalyst

GHSV = 20000 h^{-1}, $H_2O/C = 3$, $T = 1073$ K		GHSV = 20000 h^{-1}, $O_2/C = 0.5$, $T = 1073$ K		GHSV = 20000 h^{-1}, $H_2O/C = 3$, $O_2/C = 0.5$		$O_2/C = 0.5$, $H_2O/C = 3$, $T = 1073$ K	
O_2/C	% Theoretical H_2	H_2O/C	% Theoretical H_2	T (K)	% Theoretical H_2	GHSV (h^{-1})	% Theoretical H_2
0.2	50.8	3	72.3	1023	38.1	20000	93.5
0.5	72.3	5	72.5	1073	72.3	40000	72.2
0.7	72.7			1123	96.7	80000	68.1

in catalyst loading in the reformer (about 30 to have 50% of the original activity after 5000 h on stream).

To improve the durability of reforming catalyst a third step in the development of reforming catalysts was done. With this purpose, the activity and stability of cobalt based perovskite and group VIII metals supported on cobalt-perovskite were also tested in the oxidative reforming of commercial diesel fuel. Fig. 7 compares the conversion levels and H_2/CO selectivity achieved in the oxidative reforming of commercial diesel over $LaCoO_3$ and Ru/$LaCoO_3$ catalysts. As it is observed in Fig. 7, the bare $LaCoO_3$ perovskite showed a similar deactivation profile to that observed for Pt/doped alumina with the hydrogen yield decreasing with time-on-stream (a 40% decrease during the 65 h test). In contrast with bare perovskite, the activity of Ru/$LaCoO_3$ catalyst remained high and stable throughout the 80 h of reaction. An excellent hydrogen yield (90%, in relation to the maximum theoretical value, including the produced from CO by WGS) during the entire 80 h of the oxidative reforming of commercial diesel was obtained over this catalyst formulation. The activity and stability results achieved over this catalyst were similar to the best results in diesel reforming published in open literature [4]

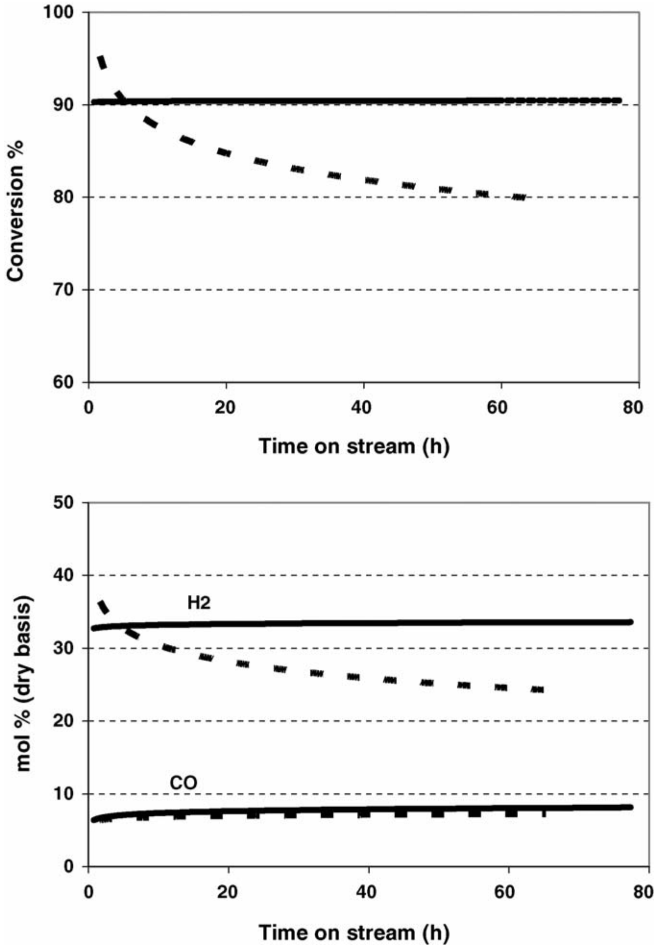

Fig. 7. Stability in the oxidative reforming of commercial diesel (15 S ppm) over: (- - -) lanthana based perovskite and (—) noble metal supported on lanthana perovskite. Reaction conditions: $T = 1123$ K, $P = 0.1$ MPa, O_2/C = 0.5, H_2O/C = 3, GHSV = 20,000 h^{-1}.

3.1.2. Water gas shift tests

In spite of the high activities reported for gold-based WGS catalysts [5–7], the Au-catalysts prepared in the project showed a catalytic activity much lower than Pt counterparts independently of the support (reducible or non reducible) and methodology of preparation used (impregnation, coprecipitation or deposition–precipitation). This fact agrees with previous results in literature [16] showing the higher activity of Pt catalysts respect to Au catalysts on equivalent loading basis. As consequence of that, the subsequent developments on WGS catalysts were based on platinum as active element. The effect of the nature of the support (Al_2O_3, CeO_2, TiO_2 and mixed CeO_2–TiO_2) on catalytic performance was investigated over platinum catalysts with the same metal loading (0.5 wt.%). Fig. 8 compares the CO conversion achieved in the WGS reaction over the Pt catalysts. Pt/TiO_2 sample is considerably more active than the Pt/CeO_2 counterpart but shows low stability at high temperatures that implies a decreasing in its WGS activity for temperatures higher than 573 K. The higher CO conversion observed for the sample supported on TiO_2 respect to that achieved on CeO_2 is an important aspect to highlight taking into account that Pt/CeO_2 catalysts are considered in literature as one of the most effective catalysts for WGS [17,18]. Pt deposited on mixed CeO_2–TiO_2 support (Pt/MO) shows better thermal stability respect to bare TiO_2 support and higher WGS activity than those corresponding to ceria and titania supports.

Optimal operational conditions for Pt/MO catalyst were determined studying the effect of temperature and space velocity on WGS activity. Fig. 9 shows the WGS performance of Pt/MO catalysts at three different residence times in the 500–600 K range temperature. Since carbon monoxide concentrations as high as 1% are tolerated by PROX catalysts, a single WGS reactor with Pt/MO catalyst operating at 300 °C and GHSV of 21,000 h^{-1} might be sufficient. The WGS reactor

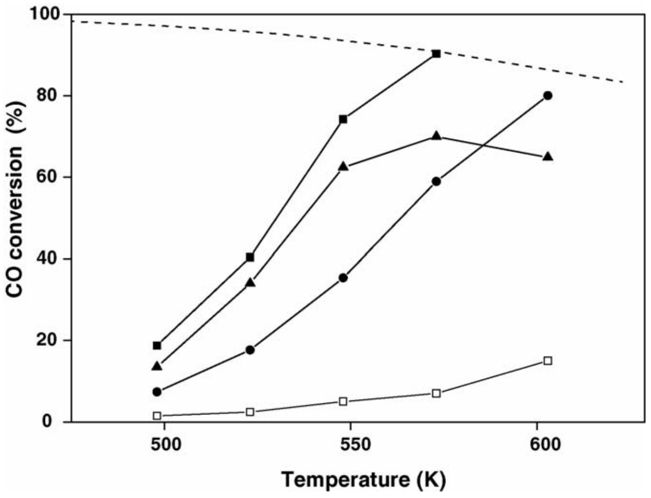

Fig. 8. WGS activity of platinum based catalysts deposited on: (□) Al_2O_3, (●) CeO_2, (▲) TiO_2 and (■) mixed oxides (MO). Reaction conditions: total pressure 1 atm, GHSV = $21,200\ L\ h^{-1}\ kg_{cat}^{-1}$; feed gas composition: H_2 28 vol.%, CH_4 0.1 vol.%, CO 4.4 vol.%, CO_2 8.7 vol.%, N_2 29.2 vol.%, H_2O 29.6 vol.%. Dotted line shows thermodynamic equilibrium limit.

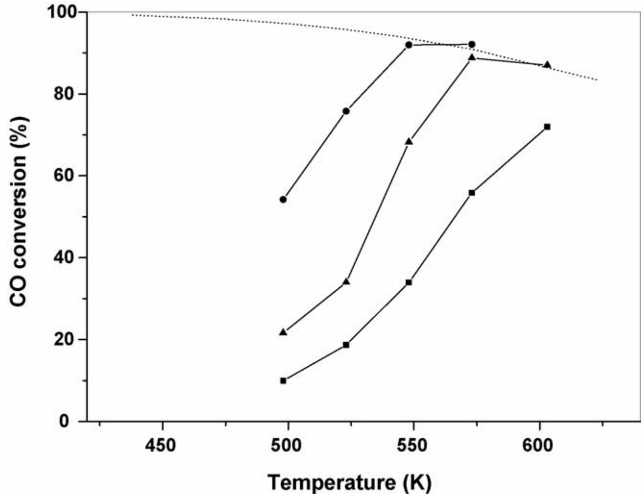

Fig. 9. Effect of reaction temperature and space velocity on CO conversion by WGS over Pt/MO catalyst: (■) 42, 400 L h^{-1} kg_{cat}^{-1}, (▲) 21, 200 L h^{-1} kg_{cat}^{-1} and (●) 10, 600 L h^{-1} kg_{cat}^{-1}. Reaction conditions: total pressure 1 atm; feed gas composition: H_2 28 vol.%, CH_4 0.1 vol.%, CO 4.4 vol.%, CO_2 8.7 vol.%, N_2 29.2 vol.%, H_2O 29.6 vol.%. Dotted line shows thermodynamic equilibrium limit.

working under these conditions can reduce the CO concentration from 6.0 to about 0.5 vol.%. The stability of Pt/MO catalysts under WGS condition was also evaluated in a 100 h long stability test at 573 K and a space velocity of 21,000 h^{-1}. CO conversion versus time-on-stream is shown in Fig. 10. As it is observed in Fig. 10, the Pt/MO catalyst shows a good stability under real working conditions maintaining a CO conversion level higher than 90% over the 100 h of duration of the experiment.

3.1.3. Preferential oxidation tests

The first set of screening results over Pt and Au catalysts supported on Al_2O_3, ZSM-5, TiO_2 and CeO_2–Al_2O_3 indicated that the catalysts based on platinum were more active than those based on gold for all supports and methodologies of preparation used. For that reason we concentrate the following PROX developments only on platinum-based catalysts.

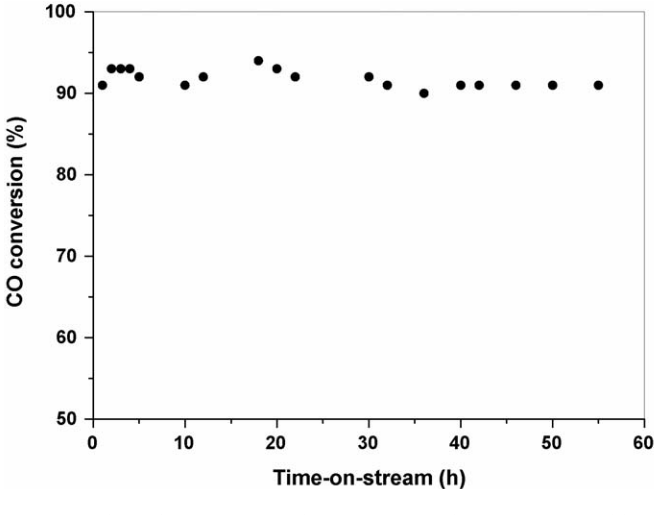

Fig. 10. Stability of Pt/MO catalyst for the WGS reaction. Reaction conditions: total pressure 1 atm, T = 573 K, GHSV = 21, 200 L h^{-1} kg_{cat}^{-1}; feed gas composition: H_2 28 vol.%, CH_4 0.1 vol.%, CO 4.4 vol.%, CO_2 8.7 vol.%, N_2 29.2 vol.%, H_2O 29.6 vol.%.

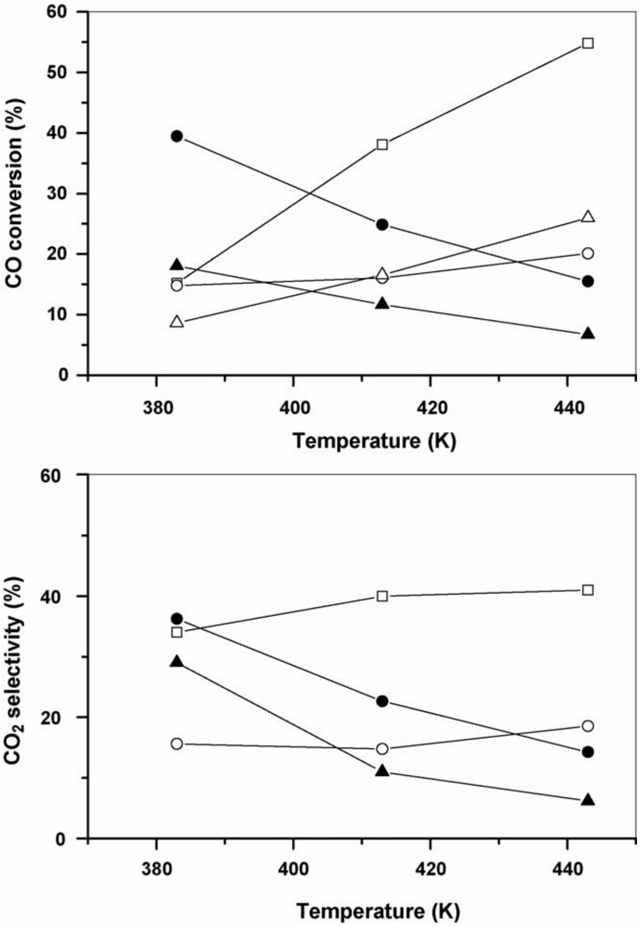

Fig. 11. PROX reaction over platinum based catalysts supported on: (□) Al_2O_3, (●) CeO_2, (○) Ce-doped Al_2O_3, (▲) TiO_2 and (■) zeolite ZSM-5. Reaction conditions: total pressure 1 atm, GHSV = 13, 000 L h^{-1} kg_{cat}^{-1}, O_2/CO = 0.5; feed gas composition (mol%): H_2 43.9, CO 0.6, CO_2 17.0, N_2 balance.

The influence of the support used to disperse platinum metal (1 wt.%) on the conversion of CO at various temperatures is presented in Fig. 11. As it is observed in Fig. 11, the sample supported on Al_2O_3 (Pt/A) showed the better results in activity and selectivity for CO oxidation at temperatures higher than 413 K.

In a third step, it was determined the optimal metal loading and operation conditions of platinum supported on alumina catalysts evaluating the effect on the CO conversion of O_2/CO feed ratio, the presence of water in the feed, temperature and overall gas flows. As representative example of this study, Fig. 12 shows plots of CO conversion and CO_2 selectivity at various O_2/CO feed ratios as a function of reaction temperature for Pt/A catalyst. As it is observed in Fig. 12 the CO conversion increases and selectivity towards the formation of CO_2 decreases as O_2/CO increases. However, the effect of the oxygen excess is much more pronounced on the CO oxidation. As a result, higher CO oxidation rates may be obtained, and therefore lower amount of catalyst loaded in the

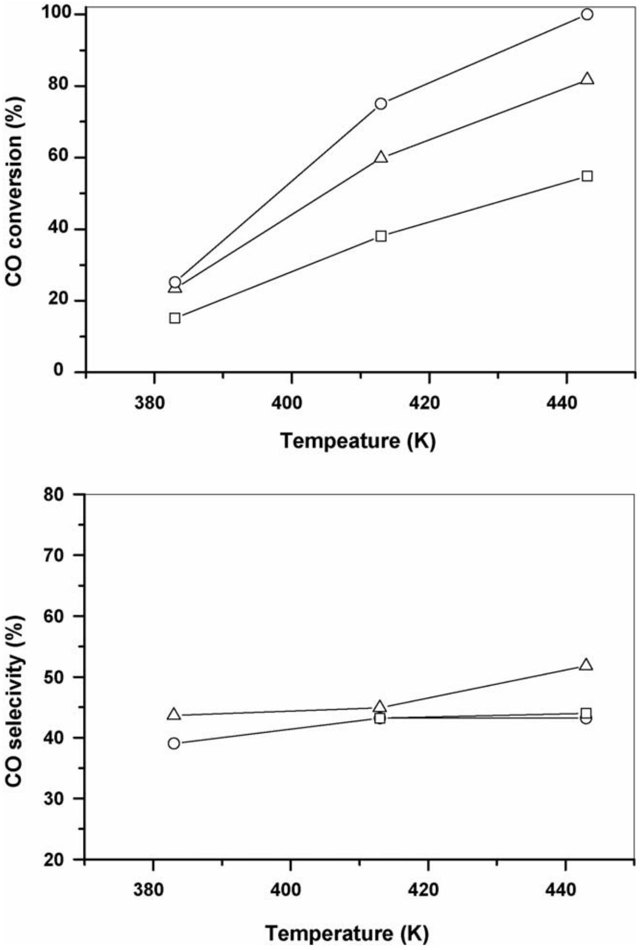

Fig. 12. Effect of reaction temperature and O_2/CO feed ratio on CO conversion and selectivity by PROX over Pt/Al_2O_3 catalysts: (○) O_2/CO = 0.5, (△) O_2/CO = 0.8 and (□) O_2/CO = 1.1. Reaction conditions: total pressure 1 atm, GHSV = $13{,}000\,L\,h^{-1}\,kg_{cat}^{-1}$; feed gas composition (mol%): H_2 43.9, CO 0.6, CO_2 17.0, N_2 balance.

PROX unit, without an excessive loss in selectivity, working with O_2/CO near to 1.0. To complete the study conducting to the determination of the operation parameters that simulate the operation of catalyst in PROX system, studies covering the influence of water and space velocity on CO conversion and selectivity were also performed. As consequence of these studies, the operational conditions for the developed PROX catalyst were derived (O_2/CO feed ratio of 1.3, GHSV of $2900\,h^{-1}$ and temperature of 443 K) in order to reduce the CO concentration to values below 50 ppm in a gas stream simulating the gas mixture after the WGS unit (H_2 33.4 vol.%, CO 0.4 vol.%, CO_2 12.9 vol.%, N_2 31.6 vol.%, H_2O 21.7 vol.%).

The stability of platinum based catalyst under above conditions was also determined. Fig. 13 shows the CO conversion and selectivity for a 50 h long-term test. It is clear from data in Fig. 13, that the catalyst, after a period of stabilization in the initial 5 h of operation in which its activity increases from a CO of 85–100%, exhibited a very stable behaviour with high performance (conversion higher than 99.5%) during the entire period of the long-term test PROX reaction.

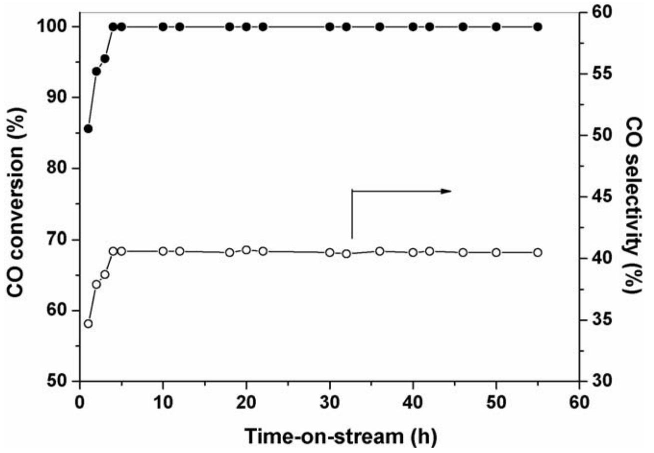

Fig. 13. Stability of Pt/Al_2O_3 catalyst for the PROX reaction. Reaction conditions: total pressure 1 atm, GHSV = $2850\,L\,h^{-1}\,kg_{cat}^{-1}$, O/CO = 1.3; feed gas composition (mol%): H_2 33.4, CO 0.46, CO_2 12.9, H_2O 21.7, N_2 balance.

3.2. Preliminary reformer testing results

In Fig. 14 medium temperatures of each reactor (Tm OSR, Tm WGSR and Tm PROX) and gas composition at the fuel processor outputs is presented. It can be observed three regions. In zone 1, only the OSR is working; in zone 2 the WGS reactor is added, so an increase of H_2 and CO_2 and a decrease of N_2 and CO is observed; in zone 3 it is finally connected the PROX, so a slight reduction in the H_2 percentage and an important one in the CO percentage (levels lower than 100 ppm) are achieved.

It can be observed a stable operation of the set at around 800–850 °C in the OSR, 270–300 °C in the WGS reactor, and 165–180 °C in PROX reactor.

The stream gas composition at the output of the fuel processor was 40–44% of H_2, 18–20% CO_2. CO concentration is approximately about 7.4% in the OSR, between 0.3% and 1% at the output of the WGS reactor and less than 100 ppm at the output of the PROX. All compositions are in dry basis and it is expected to detect a composition of CO lower than 10 ppm once an adequate measuring system of gas stream compositions will be installed for a proper measurement of such value.

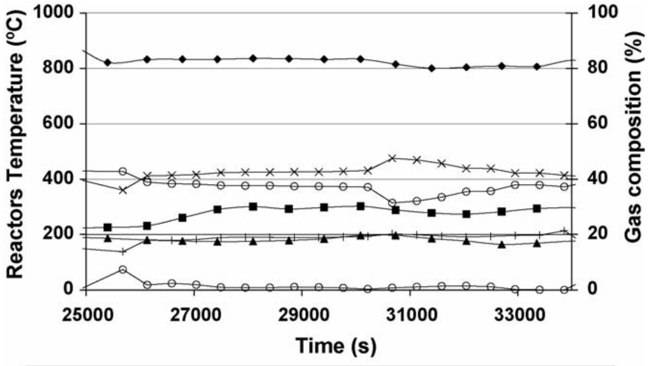

Fig. 14. Diesel reformer preliminaries results: temperature evolution and gas stream composition.

4. Conclusions

The whole system is going to be operated following a defined test plan. First operational results will be obtained in the last months of 2005 and evaluated during first months of 2006. Evaluation system results will feedback the process design to improve the system from an operational and energy point of view taking in mind the future design, construction and operation of a 25 kW system able to full fit operational requirements as mobile power source.

References

[1] J.C. Amphlett, R.F. Mann, B.A. Pepley, P.R. Roberge, A. Rodrigues, J.P. Salvador, J. Power Sources 71 (1998) 179.

[2] A.F. Ghenciu, Curr. Opin. Solid State Mater. Sci. 6 (2002) 389.

[3] M. Krumpelt, T.R. Krause, J.D. Carter, J.P. Kopasz, S. Ahmed, Catal. Today 77 (2002) 3.

[4] D.J. Lin, M. Krumpelt, Int. J. Appl. Ceram. Technol. 2 (4) (2005) 301.

[5] T. Utaka, T. Okanishi, T. Takeguchi, R. Kikuchi, K. Eguchi, Appl. Catal. A: Gen. 245 (2003) 343.

[6] W. Wang, R.J. Gorte, J.P. Wagner, J. Catal. 212 (2002) 225.

[7] Q. Fu, A. Weber, M.F. Stephanopoulos, Catal. Lett. 77 (1–3) (2001) 87.

[8] S.H. Oh, R.M. Sinkevithc, J. Catal. 142 (1993) 254.

[9] M. Haruta, M. Date, Appl. Catal. A: Gen. 222 (2001) 427.

[10] J.B. Wang, S. Lin, T. Huang, Appl. Catal. A: Gen. 232 (2002) 107.

[11] F. Tinaut, D. Sopeña, A. Horrillo, Y. Briceño, F. Rosa, Simulation model to design a diesel autothermal fuel processor prototype, in: Proceeding of the 15th WHEC, June, Yokohama (Japan), 2003.

[12] F. Rosa, Y. Briceño, C. Bordons, R. Navarro, Desarrollo de un reformador diesel para producción de hidrógeno y uso en una pila de combustible tipo PEM, in: Proceeding of the Second EHEC, October 2005.

[13] D. Sopeña, A. Horrillo, Y. Briceño, F. Rosa, Modelado de un reformador de gasóleo para alimentar una pila de combustible de 5 kW, in: XVI Congreso Nacional de Ingeniería Mecánica, December, León (Spain), 2004.

[14] F.V. Tinaut, A. Horrillo, Y. Briceño, D. Sopeña, M.E. Herráiz, Modelo para la simulación del proceso de obtención de hidrógeno mediante el reformado de gas natural, in: III Jornadas Nacionales de Energía Termodinámica, June, Valencia (Spain), 2003.

[15] F. Rosa, Y. Briceño, C. Bordons, R. Navarro, Energía (2005) 11.

[16] G. Jacobs, S. Ricote, P.M. Patterson, U.M. Graham, A. Dozier, S. Khalid, E. Rodhus, B.H. Davis, Appl. Catal. 295 (2005) 229.

[17] S. Luegnaruemitchai, E. Osuwan, Gulari, Catal. Commun. 4 (2003) 215.

[18] G. Jacobs, E. Chenu, P.M. Patterson, L. Williams, D. Sparks, G. Thomas, B.H. Davis, Appl. Catal. A: Gen. 258 (2004) 2003.